Journal of Alloys and Compounds 515 (2012) 123–127

Contents lists available at SciVerse ScienceDirect

Journal of Alloys and Compounds

journal homepage: www.elsevier.com/locate/jallcom

Solidifying incongruently melting intermetallic phases as bulk single phases using the example of Al_2Cu and Q-phase in the Al–Mg–Cu–Si system

Andrea Löffler[a], Joachim Gröbner[b], Milan Hampl[b], Hannes Engelhardt[a], Rainer Schmid-Fetzer[b], Markus Rettenmayr[a,*]

[a] Institute of Materials Science and Technology, Friedrich-Schiller-University, Jena, Germany
[b] Institute of Metallurgy, Clausthal University of Technology, Clausthal-Zellerfeld, Germany

ARTICLE INFO

Article history:
Received 27 September 2011
Received in revised form
15 November 2011
Accepted 23 November 2011
Available online 2 December 2011

Keywords:
Phase diagrams
Intermetallics
Thermodynamic modeling
Thermal analysis
Liquid–solid reaction

ABSTRACT

Plane front directional solidification experiments were carried out for preparing incongruently melting intermetallic phases in the quaternary alloy system Al–Cu–Mg–Si, particularly the binary Al_2Cu phase and the quaternary phase ("Q-phase"). By this method, bulk samples that consist of only a single phase are generated. Sample sections consisting of 100% single phase Al_2Cu and of 95% Q-phase, respectively, were obtained. The composition of the Q-phase was measured by Energy Dispersive X-ray Spectroscopy (EDX). The measured concentrations are close to the $Al_3Cu_2Mg_9Si_7$ composition that has recently been predicted as most stable by *ab initio* calculations. A peritectic temperature of 703 °C for the reaction $Q \rightarrow L + Mg_2Si + (Si)$ was determined by differential scanning calorimetry (DSC). An optimization of the Calphad database was performed considering the measured composition and peritectic temperature. For validating the optimized database, Scheil calculations were performed and compared with the experimentally determined sequence of solidifying phases.

1. Introduction

Al based alloys in the system Al–Cu–Mg–Si are widely used, *e.g.* in the automotive and aerospace industry. Their microstructures have been extensively optimized to achieve the mechanical and electrochemical properties suitable for the relevant application. For predicting the microstructure, numerous models for microsegregation formation during solidification and precipitation formation during heat treatments have been developed. The accuracy of the calculation results is not only dependent on the model itself, but also depends most sensitively on the phase diagram data used for the calculation [1]. The most commonly used state-of-the-art approach for describing phase diagrams in multicomponent systems is the Calphad method.

Several thermodynamic descriptions of the quaternary system Al–Cu–Mg–Si have been published [2–5]. One central aspect for modeling the entire system is to find a correct description of the quaternary Q-phase. Although it is observed in technical alloys, *e.g.* in the 6xxx series, relatively little is known about this phase, *e.g.* concerning its exact composition and solubility range there is only approximate knowledge. Reported compositions vary and are given as $Al_4Cu_1Mg_5Si_4$ [6], $Al_4Cu_2Mg_8Si_7$ [7], $Al_xCu_2Mg_{12-x}Si_7$ [7], $Al_3Cu_2Mg_9Si_7$ [8] and $Al_5Cu_2Mg_8Si_6$ [9]. While $Al_5Cu_2Mg_8Si_6$ has been used in most Calphad databases, *ab initio* calculations performed by Wolverton [8] report $Al_3Cu_2Mg_9Si_7$ to be the thermodynamically most stable composition. Recently, Chang [5] modeled the Al–Cu–Mg–Si system using the $Al_3Cu_2Mg_9Si_7$ composition and achieved good agreement with enthalpies of formation from *ab initio* calculations and previous experimental data measured by Petrov et al. [10] and Zolotorevsky et al. [11]. However, little direct experimental information regarding the Q-phase is available, since it has only been obtained in small quantities by experiments carried out in the Al-rich corner of the phase diagram. Additionally, the difficulties of generating samples consisting exclusively of a single phase with a very narrow solubility range by casting or powder metallurgical processing routes has not been addressed sufficiently in former publications.

The aim of the present work is to prepare bulk intermetallic phases in the Al–Mg–Cu–Si system by plane front directional solidification in a quantity of several grams. Two incongruently melting phases with varying solubility limits are prepared with this method, particularly the θ-Al_2Cu phase and the Q-phase. EDX measurements for the composition and DSC measurements for the incongruent melting point of the Q-phase are provided as data for its composition and peritectic temperature that are used to optimize the Al–Cu–Mg–Si Calphad database.

---

* Corresponding author at: Institute of Materials Science and Technology, Friedrich Schiller University, Löbdergraben 32, 07743 Jena, Germany.
Tel.: +49 3641 947790; fax: +49 3641 947792.
E-mail address: M.Rettenmayr@uni-jena.de (M. Rettenmayr).

0925-8388/$ – see front matter © 2011 Published by Elsevier B.V.
doi:10.1016/j.jallcom.2011.11.119

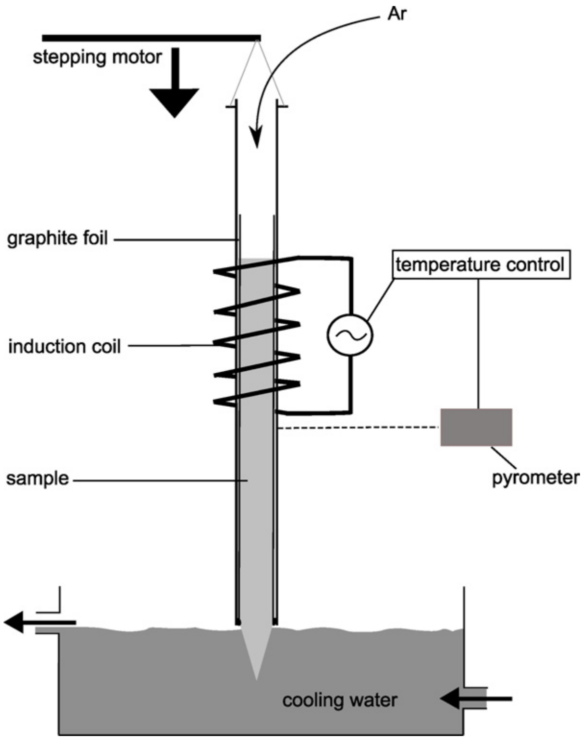

Fig. 1. Experimental set-up for plane front directional solidification. The sample is placed in a quartz tube that acts as a crucible. It is heated at the top by an induction furnace. The quartz tube is open at the bottom, allowing a fast heat transfer from the sample into the cooling water. A stepping motor lowers the sample into the cooling water. A 2-color pyrometer is used to control the temperature and to ensure a steady temperature field.

2. Experimental

2.1. Plane front directional solidification

If an alloy with the total composition of an incongruent melting intermetallic phase is solidified, there will be a primary solidifying phase which is not the intermetallic phase. The location of crystallization of the intermetallic phase will depend on the morphology of the primary phase that can generally not be suppressed. Spatial separation of the sequence of solidifying phases is possible if the sample solidifies with plane front under Scheil conditions (complete mixing in the liquid, negligible diffusion in the solid) [12]. For obtaining an intermetallic phase directly from the melt, an overall composition that differs from that of the intermetallic phase needs to be chosen. It is necessary to identify the two-phase equilibrium of the relevant phase with the melt. In the present work, a series of isopleth sections of the quaternary phase diagram was calculated using a preliminary database for identifying the relevant two-phase fields. If the overall concentration is in a concentration range in which there is an equilibrium between the liquid phase (“L”) and the intermetallic phase, this phase will solidify as primary phase (if retarded nucleation does not lead to suppression of its formation). When the temperature is lowered and the two-phase field of liquid and primary intermetallic is left, other phases will crystallize according to the relevant equilibria, leaving the bulk intermetallic phase as a certain volume fraction of the sample.

For obtaining a maximum amount of primary Q-phase, additional Scheil calculations were performed to select promising initial concentrations and to estimate the achievable phase fraction. The initial concentrations for obtaining θ-Al_2Cu were chosen so that a sufficient amount primary θ-Al_2Cu could be obtained without strongly varying the initial concentrations as compared to the Q-phase experiments. For all preliminary calculations in this work the database PanMg8 in combination with the software package “Pandat” [13] was utilized.

Considering the uncertainty in the phase diagram data, about 15 alloys (for compositions see below) with the most promising concentrations according to the preliminary calculations were prepared and cast in rods with 8 mm diameter to produce a fine equiaxed initial microstructure. The samples were cut to a length of 17 cm and a tip was machined at one end of each sample. Wrapped in graphite foil, they were placed in a quartz tube that acted as crucible. The experimental set-up is shown in Fig. 1. The samples were placed in a high frequency induction coil that serves a two-fold purpose: on the one hand it heats the sample, and on the other hand it stimulates convection in the liquid through both Lorentz forces and lateral temperature gradients. Thus, complete mixing in the melt is achieved in good approximation. The quartz tube was flooded with Ar gas for avoiding oxidation and humidity uptake. The lower end of the sample was cooled by streaming water. Thermal gradients up to $12\,K\,mm^{-1}$ were thus achieved in the sample. After a holding time of 2 h for adjusting a defined initial microstructure with a plane front [14,15], the sample was lowered into the water with a velocity of $0.3\,\mu m\,s^{-1}$. Using the above mentioned high thermal gradient and low solidification velocity, plane solidification front is achieved. Different phases which solidify with decreasing temperature are spatially separated along the solidifying length of approximately 10 cm. The solidified samples were cut in 3–4 cm long pieces, ground with SiC paper (80–4000 grain) and polished with diamond spray (0.25 μm). The microstructures were examined by SEM, and the initial concentration and the concentration of the Q-phase were measured by EDX measurements.

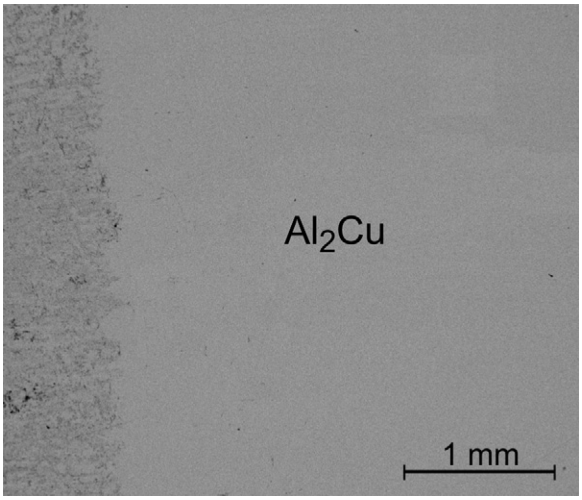

Fig. 2. Phase separation after plane front solidification in a quaternary Al–22%Cu–6.5%Mg–7.8%Si alloy with θ-Al_2Cu as primary phase; on the very left side the original cast microstructure is visible. There is no phase contrast in the directionally solidified microstructure on the right side.

2.2. DSC measurements of the peritectic formation of the Q-phase

Sample segments consisting mostly of Q-phase were cut into four disks with a thickness of 2 mm. Each disk was cut into two halves to fit the DSC alumina crucible. The disk with the highest fraction of Q-phase (~95 vol.%) was studied by differential scanning calorimetry (DSC) in a heat-flux cylindrical Calvet-type calorimetric system Multi HTC 96 (Setaram, Caluire, France). The equipment was calibrated using pure Cu, Ag and Al. He, at a flow rate of 2 l/h, was used as the analysis chamber gas. A sapphire cylinder was used as the reference material. The sapphire mass was 358.6 mg. The sample (weight 158.5 mg) was heated up to 800 °C with a heating rate of +2 K/min and then cooled down with −2 K/min. The overall uncertainty of DSC measurements for temperature determination is estimated as ±3 K. In the evaluation of transition temperatures the onset temperature was always taken. For heating cycles, the onset temperature was taken for invariant reactions and the peak maximum for all other signals.

3. Results and discussion

To investigate the method’s suitability for preparing bulk samples of incongruently melting phases, an experiment aiming at θ-Al_2Cu as primary phase was performed. The resulting microstructure of the first part of the sample is given in Fig. 2. There are no visible inclusions of other phases. Secondary phases with a length scale that is not visible in an optical microscope are not to be expected. It is thus concluded that a sample section with pure θ-Al_2Cu-phase was achieved.

3.1. Determination of the Q-phase composition

Since there was little prior knowledge concerning the accuracy of the available thermochemical database in the relevant concentration range, several orientation experiments were performed to determine adequate initial concentrations. In the following sections the results of two experiments aiming at Q-phase and one

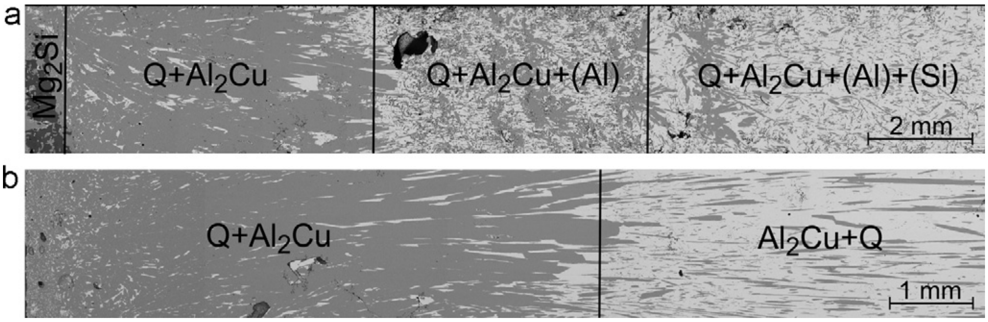

Fig. 3. Longitudinal sections of the directionally solidified samples. (a) alloy 1 and (b) alloy 2. The solidification direction is from the left to the right, where the left side of the micrographs represents the normalized sample position of zero. The overall section lengths are 2.8 cm and 2.1 cm, respectively. Sections with high fraction of Q-phase over a length of approximately 1 cm are visible in both samples.

Table 1
Initial concentrations and observed phases.

Sample #	Initial concentrations (at.%)				Observed phases
	Al	Cu	Mg	Si	
1	63.4	16	9.8	10.8	Mg_2Si, Q, θ-Al_2Cu, (Al), (Si)
2	66.5	13.5	10.2	9.8	Q, θ-Al_2Cu

aiming at θ-Al_2Cu are presented. The initial concentrations for the alloys aiming at primary solidification of the Q-phase and the phases that were detected in the first third of the solidified sample are given in Table 1. The according micrographs of the longitudinal sections of the samples are shown in Fig. 3a and b. The highest fraction of Q-phase is found in the second sample where volume fractions Q-phase of up to 95% were detected by image analysis. Parts of this sample were used in the DSC measurement to obtain the peritectic temperature. In all the samples, amount and length scale of the Q-phase were sufficient for performing EDX concentration measurements. The measured concentrations and standard deviations are given in Table 2. In available thermochemical databases the Q-phase is simplified as a stoichiometric phase with no solubility range. To verify this simplification, measurements were performed in different samples in which the Q-phase was in equilibrium with the Mg_2Si, θ-Al_2Cu, (Al) and (Si) phases, respectively. If the Q-phase had a solubility range, the concentrations should vary, depending on the neighboring phase. However, in the >20 measurements which were performed in the various samples no such dependence was observed. The variation of all measured concentrations is ±0.6 at.% for Mg and even lower for Al, Cu and Si. Variations in this order of magnitude are due to statistical errors in the EDX measurement. It is concluded that the Q-phase has indeed a negligible solubility range, and describing the Q-phase as a stoichiometric phase in a detailed Calphad evaluation is expedient. Comparing the results with the compositions reported in the literature, the best agreement can be found with the $Al_3Cu_2Mg_9Si_7$ composition as predicted by Wolverton [8]. For the other compositions proposed in the literature, the Mg content is underestimated and the Al content is overestimated.

Table 2
Comparison of measured Q-phase compositions and compositions reported in the literature.

Composition	Al	Cu	Mg	Si	Ref.
Measured	16.8 ± 0.5	9,1 ± 0.3	44.3 ± 0.6	29.8 ± 0.3	This work
$Al_3Cu_2Mg_9Si_7$	14.3	9.5	42.9	33.3	[8]
$Al_5Cu_2Mg_8Si_6$	23.8	9.5	38.1	28.6	[9]
$Al_4Cu_2Mg_8Si_7$	19.0	9.5	38.1	33.3	[7]
$Al_4CuMg_5Si_4$	28.6	7.1	35.7	28.6	[6]

3.2. *Determination of the peritectic temperature*

Events obtained from the thermal analysis, as extracted from the DSC signals, are given in Table 3. In the first heating cycle, the peritectic reaction of the Q-phase is indicated by a strong sharp signal at 703 °C. Heating of the sample was stopped below the liquidus temperature to avoid total melting of the sample. During the following cooling cycle, the peritectic reaction started 38 K lower at 665 °C. The additional signal can also be assigned to calculate effects of the phase diagram (see Table 3 and Fig. 4). The interpretations of the experimental temperatures in the last two columns are based on the present thermodynamic calculation.

During the measurement, the sample crucibles changed their color to a light gray shade, probably by minor evaporation of Mg or any other elements. Although the sample was not melted completely, its form changed to more rounded and matt surface. Therefore only the first heating cycle was used for evaluation.

3.3. *Calculation of the formation of the Q-phase*

After detecting the correct composition for the Q-phase (see Section 3.1) and measuring the peritectic reaction temperature, the parameters of the Q-phase in the Calphad description were adjusted to these data. Existing thermodynamic descriptions of the quaternary Al–Cu–Mg–Si system by Pan et al. [4] and Chang et al. [5] are based on the available experimental data by [10] and

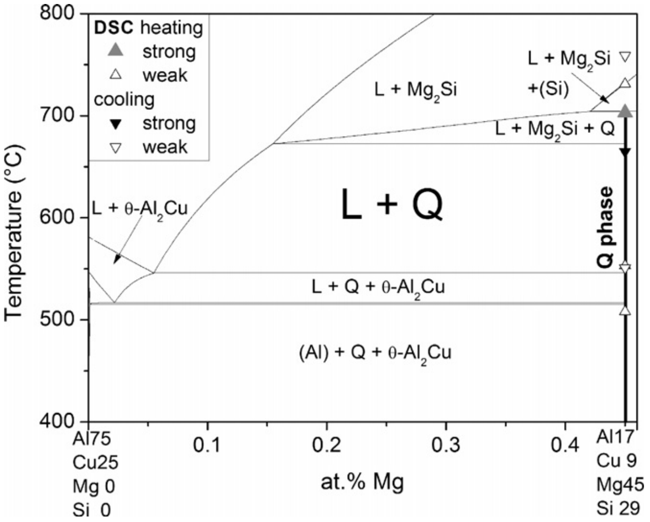

Fig. 4. Calculated vertical section of the quaternary system Al–Cu–Mg–Si from $Al_{75}Cu_{25}$ to the composition of the Q-phase $Al_{17}Cu_9Mg_{45}Si_{29}$ (at.%). Measured DSC signals are included as triangles.

Table 3
Temperatures extracted from the DSC signals obtained by thermal analysis of the Q-phase sample.

Thermal signal (°C)		Interpretation from equilibrium calculation	
Heating[a]	Cooling[b]	Calculation (°C)	Phase boundary (at upper temperature limit)
		923	L/L + Mg_2Si
731 w	759 w	732	/L + Mg_2Si + (Si)
703 s	665 s	703	P: L + Mg_2Si + (Si) → Q
553 w	551 w	545	/L + Q + θ-Al_2Cu
		517	/L + Q + θ-Al_2Cu + (Al)
508 w		515	/Q + θ-Al_2Cu + (Al)

[a] Onset for invariant reactions, peak maximum otherwise.
[b] Onset (s, strong signal; w, diffuse signal).

[11]. These data give only some equilibria with the Q-phase in the Al-rich corner of the quaternary system (Al > 60 wt.%). Direct experimental information on the Q-phase has not been available so far. The measured peritectic reaction temperature is therefore a crucial information to fix the Gibbs energy of the Q-phase which is Mg-rich and contains only 17 at.% Al. The new description of the Gibbs energy is

$$G^{0,Q}_{\mathrm{Al:Cu:Mg:Si}} = -45380 + 23.6 \times T + 0.17G^{0,\mathrm{FCC}}_{\mathrm{Al}} + 0.09G^{0,\mathrm{FCC}}_{\mathrm{Cu}} + 0.45G^{0,\mathrm{HCP}}_{\mathrm{Mg}} + 0.29G^{0,\mathrm{diamond}}_{\mathrm{Si}}$$

Adjusting the parameters for the Q-phase affects the phase equilibria of the Al-rich compositions only marginally. The phase equilibria measured by [10] and [11] are mainly determined by the subsystems, especially the ternary Al–Mg–Si. This fact is even more pronounced for the isothermal phase analysis of the Al-rich corner given by Axon [16,17] and Smith [18].

For the composition of the Q-phase, the authors of Ref. [5] chose the same value that we found in this work and evaluate an enthalpy of formation for the Q-phase between −16.1 and −17.6 kJ/mol-atoms, as given by [4,8,19] in their calculations. The enthalpy of formation of the Q-phase in this work (−17.1 kJ/mol-atoms) fits well in this range. For the $Al_5Cu_2Mg_8Si_6$ composition of the Q-phase, the enthalpy of formation by [5] and [8] is reported to be between −12.0 and −12.9 kJ/mol-atoms.

Fig. 4 shows the calculated vertical section of the quaternary system Al–Cu–Mg–Si from $Al_{75}Cu_{25}$ to the composition of the Q-phase $Al_5Cu_2Mg_8Si_6$ (at.%). Measured DSC signals are included as triangles. The key signal for the optimization, particularly the peritectic reaction temperature of the Q-phase, is given in gray. The expansion of the L + Q field is illustrated by an overlay of four calculated vertical sections between $Al_{70}Cu_{30}$ and $Al_{85}Cu_{15}$ to the composition of the Q-phase (Fig. 5). All sections meet in the Q-phase on the right side from different start points in the Al–Cu subsystem on the left side. The extension of the L + Q field is given by arrows.

3.4. Comparison with solidification experiments

In the plane front solidification experiment, the length of the solidifying sample is substantially longer than the solid diffusion distance during the solidification time. Solid state back diffusion has therefore only negligible influence on the solidification path. Complete mixing in the melt combined with negligible diffusion in the solid leads to solidification conditions that are essentially the Scheil conditions. Therefore the liquid composition should follow the solidification path that is predicted by Scheil calculations if plane solidification front is achieved. Using this assumption, Zhao and Rettenmayr [12] successfully tracked the solidus and liquidus lines in the binary Al–Zn system with the same experimental set-up.

The thermochemical parameter set obtained with the more detailed information about the Q-phase was used to calculate Scheil solidification paths of the investigated alloys. The calculated phase amounts of each individual step versus the normalized sample length of the different alloys are given in Fig. 6a and b (note that the units in the calculation are at.%/at.% and have not been converted to volumetric units, since a direct comparison of volume fractions in the experiment is not in the scope of this paper). As the longitudinal sections in Fig. 3 represent approximately the first third of the solidified samples, the observed phases can be qualitatively compared with the calculation results for a normalized length up to 0.3. All phases which were predicted by the Scheil calculations are also observed in the samples and appear in the predicted order.

According to the calculations, a region of pure Q-phase is to be expected in the first part of the sample. However, the micrographs show that while there is a region with a high fraction of Q (>90%) it has not formed purely, but with small inclusions of θ-Al_2Cu. In several experimental runs with slightly varied initial compositions, crystallization of pure Q-phase was attempted, but never achieved. On the other hand, the experiment aiming at θ-Al_2Cu shows that the method presented in this paper is suitable to prepare bulk samples of incongruently melting phases. The different solidification behavior of Q and θ-Al_2Cu can be ascribed to two facts: unlike θ-Al_2Cu the Q-phase is prone to faceted growth and has a very narrow solubility range. The former leads to destabilization of the plane solidification front and to the formation of θ-Al_2Cu between the Q domains and the latter impedes homogenization while the sample is cooled with a slow cooling rate.

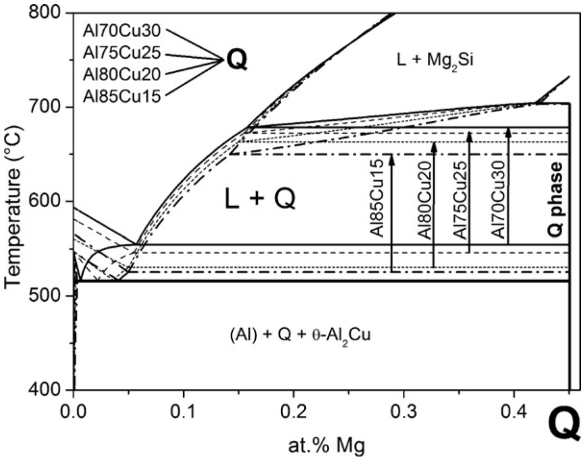

Fig. 5. Calculated overlay of vertical sections of the quaternary Al–Cu–Mg–Si phase diagram from four different compositions along the Al–Cu edge to the Q-phase composition. The extension of the L + Q field is illustrated by arrows. According to the temperature and concentration range of the L + Q field, the initial concentrations of the sample concentration in the directional solidification experiments were chosen.

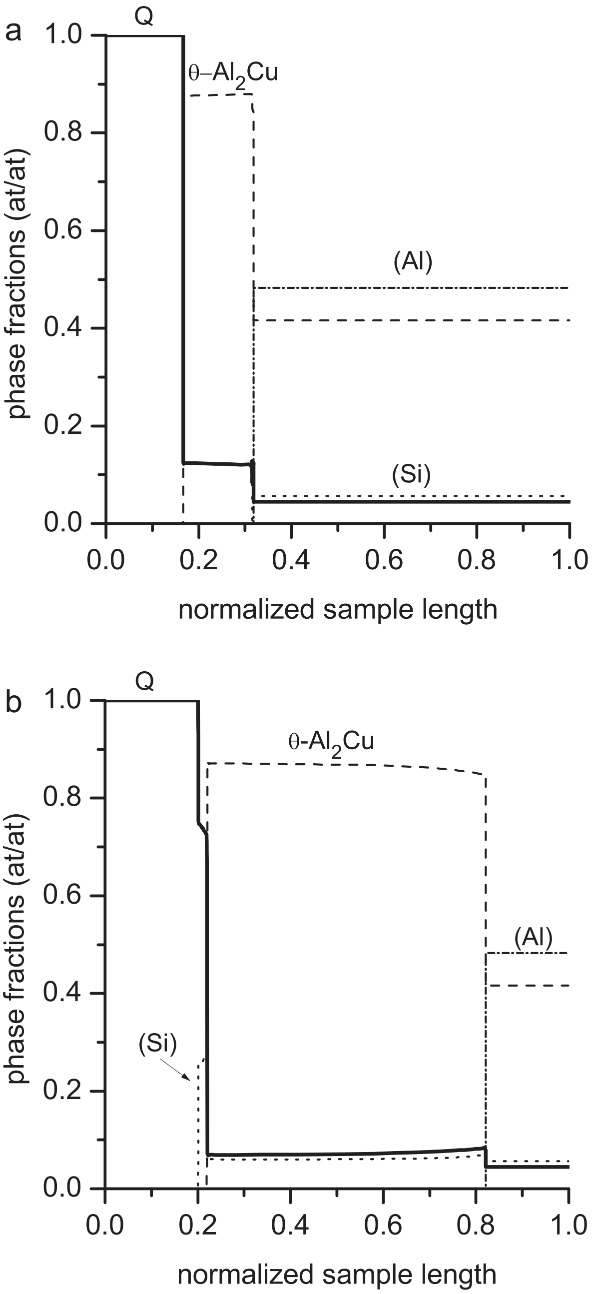

Fig. 6. Results of Scheil type calculations: calculated phase fractions versus the normalized sample lengths of (a) alloy 1 and (b) alloy 2.

Further work will aim at perfecting the fraction of Q-phase by modifying the experimental equipment (temperature gradient, stimulated convection) and experimental procedure (start with precisely defined initial conditions through long holding periods before the directional solidification experiment). Pure bulk Q-phase will be investigated by X-ray diffraction and will be used to determine its enthalpy of formation by DSC measurements, and the thermodynamic parameter set of the Al–Cu–Mg–Si phase diagram will be further optimized in a larger concentration range.

4. Conclusions

- The incongruent melting intermetallic compound θ-Al_2Cu has been produced as single phase with several cm in length and with a sample size of 8 mm diameter.
- Macroscopic amounts of Q-phase have been prepared using plane front solidification. Its chemical composition has been investigated and measured as $Al_{17}Cu_9Mg_{44}Si_{30}$ which is in good agreement with the $Al_3Cu_2Mg_9Si_7$ stoichiometry proposed by [8]. No significant solubility range was detected.
- The peritectic temperature of the Q-phase has been measured as 703 °C by DSC measurements.
- A new thermochemical parameter set for the Q-phase has been assessed using the new composition and peritectic temperature. Scheil solidification calculations using the new parameter set were compared with the observed microstructure after the plane front solidification experiments. The phases that were predicted by the Scheil calculations were also observed in the experiment.

Acknowledgements

This research work is supported by Deutsche Forschungsgemeinschaft under grants RE1261/7 and Schm 588/35.

References

[1] M. Rappaz, M. Rettenmayr, Curr. Opin. Solid State Mater. Sci. 3 (1998) 275–282.
[2] X.Y. Yan, Y.A. Chang, F.Y. Xie, S.L. Chen, F. Zang, S. Daniel, J. Alloys Compd. 320 (2001) 151.
[3] V. Raghavan, J. Phase Equilib. Diffus. 28 (2007) 198–200.
[4] X. Pan, J. Morral, H. Brody, J. Phase Equilib. Diffus. 31 (2010) 144–148.
[5] K. Chang, S. Liu, D. Zhao, Y. Du, L. Zhou, L. Chen, Thermochim. Acta 512 (2011) 258–267.
[6] J. Lacaze, G. Lesoult, O. Relave, I. Ansara, J.P. Riquet, Z. Metallkd. 78 (1987) 141–150.
[7] L. Arnberg, B. Aurivillius, Acta Chem. Scand. A 34 (1980) 1–5.
[8] C. Wolverton, Acta Mater. 49 (2001) 3129–3142.
[9] G. Phragmen, J. Inst. Met. 77 (1950) 489–552.
[10] D.A. Petrov, N.D. Nagorskaya, Zh. Obshch. Khim. 19 (1949) 1994–2037.
[11] V.S. Zolotorevsky, N.A. Belov, M.V. Glazoff, Casting Aluminum Alloys, Alcoa Technical Center, Philadelphia, 2007.
[12] G. Zhao, M. Rettenmayr, J. Cryst. Growth 279 (2005) 540–550.
[13] S.L. Chen, S. Daniel, F. Zhang, Y.A. Chang, X.Y. Yan, F.Y. Xie, R. Schmid-Fetzer, W.A. Oates, Calphad 26 (2002) 175–188.
[14] M. Buchmann, M. Rettenmayr, J. Cryst. Growth 284 (2005) 544–553.
[15] U. Bösenberg, M. Buchmann, M. Rettenmayr, J. Cryst. Growth 304 (2007) 281–286.
[16] H.J. Axon, J. Inst. Met. 81 (1952) 209–213.
[17] H.J. Axon, J. Inst. Met. 81 (1952) 449–450.
[18] D.P. Smith, Metallurgia 63 (1962) 223–230.
[19] C. Ravi, C. Wolverton, Acta Mater. 52 (2004) 4213–4227.